# Receive Spatial Modulation Aided Simultaneous Wireless Information And Power Transfer With Finite Alphabet

Yizhe Zhao, *Student Member, IEEE*, Jie Hu, *Member, IEEE*, Anna Xie, Kun Yang, *Senior Member, IEEE* and Kai-Kit Wong, *Fellow, IEEE*

**Abstract**

As the number of communication devices rapidly grows, limited radio resources hardly accommodate the every-increasing tele-traffic. As a remedy, spatial modulation (SM) is capable of modulating additional information onto the index of transmit or receive antennas, which results in substantial improvement of spectrum efficiency. Moreover, radio frequency (RF) signal based simultaneous wireless information and power transfer (SWIPT) has attracted tremendous research interest, in order to relieve the energy-thirst of massively deployed low-power communication devices. In this paper, a receive spatial modulation (RSM) aided SWIPT system with finite alphabets is studied, in which three different transmission schemes are proposed, namely the general scheme, the superimposed scheme and the distinct scheme. Furthermore, the performance of these transmission schemes in the RSM aided SWIPT system is theoretically analysed. The energy harvested by the receiver is then maximised by jointly optimising the transmit power of the information signal and the covariance matrix of the energy signal as well as the power splitting ratio, while satisfying the quality of service of the wireless information transfer. At last, simulation results validate our theoretical analysis, while they also demonstrate that the distinct scheme has the best SWIPT performance among these three transmission schemes.

**Index Terms**

Receive spatial modulaton, SWIPT, MIMO, transceiver design, finite alphabet

# I. INTRODUCTION

## A. Background

In the era of Internet of Things (IoT), low-power communication devices are massively deployed in wireless networks. Accommodating ever-increasing number of communication devices in limited spectral bands poses great challenges for communication engineers [1]. As one of the most successful wireless communication technique in the past two decades, multiple-input-multiple-output (MIMO) system [2] [3] is capable of substantially improving the spectrum efficiency, which benefits from the spatial diversity and spatial multiplexing gains of multiple transmit and receive antennas. Recently, index modulation has attracted much research interest, since it is capable of modulating additional information on the index of sub-carriers [4] and antennas [5]. Comparing to the conventional method of modulating information on the amplitude and phase of radio-frequency (RF) signals, index modulation creates another degree of freedom to substantially improve spectrum- and energy-efficiency, while maintaining a low hardware complexity.

As a result, spatial modulation (SM) [6] [7] becomes the most popular index modulation technique. SM is constituted by both conventional modulator and spatial modulator. In the conventional modulator, such as QPSK and QAM, information bits are modulated by different amplitudes and phases of carrier signals. The modulated symbol is then transmitted by a single antenna or a group of antennas, while others are inactive. The index (or indices) of the activated antennas engaged in transmitting (or receiving) the conventionally modulated symbol is capable of carrying additional information bits. Modulating information bits by the index of antennas is known as the spatial modulator. Obviously, only activating limited antennas for transmitting conventionally modulated symbols sacrifice some of the diversity and multiplexing gains [8]. However, it substantially reduces the hardware complexity of the MIMO system, especially when it evolves to massive MIMO. Generally, SM is classified into transmit spatial modulation (TSM) [9] and receive spatial modulation (RSM) [10]. Specifically, TSM modulates information

bits by the index of the activated antennas transmitting conventionally modulated symbols, while RSM modulates information bits by the index of the activated antennas receiving conventionally modulated symbols. TSM is capable of achieving a higher spectrum efficiency than RSM, since a powerful transmitter always has more antennas than a receiver. However, RSM is more suitable for low-power communication devices, due to its low hardware complexity on the receiver side.

Apart from the spectrum scarcity, extending the life-time of the battery powered communication devices is crucial for reducing the maintenance cost of IoT. Since some of the devices are deployed in human-unreachable places, it is impractical to frequently replace their embedded batteries. RF signals can be then exploited for far-field wireless power transfer (WPT) [11]. However, conventional wireless information transfer (WIT) has already resided in RF bands. Coordinating both WPT and WIT in the same bands yields simultaneous wireless information and power transfer (SWIPT). Normally, received RF signals are split into two portions either in the time domain or in the power domain by receivers [12]. One portion of received RF signals is for energy harvesting and the other for information decoding. Therefore, the WIT and WPT performance can be adaptively adjusted in order to satisfy distinct requirements of receivers.

In an SM system, information signals are targeted on a limited number of antennas of either the transmitter or the receiver activated for WIT. In order to increase its WPT capability, dedicated energy signals can be targeted on the rest of antennas, which do not carry any information [13]. By carefully controlling the power of energy signals, the receiver is still capable of recognising the indices of antennas activated for WIT. The tradeoff of WIT and WPT can be obtained by adjusting either the number of antennas activated for WIT and WPT or by adjusting the transmit power of modulated information signal and dedicated energy signal.

### *B. Related Works*

SM has already been widely studied for years in the past decades [9], [10], [14]–[19]. Specifically, in [14], an iterative algorithm was proposed to maximise the Shannon capacity of SM by optimising the activation probability of transmit antennas. Moreover, Wu *et al.* [17]

studied an transmission optimized spatial modulation (TOSM) by adopting the adaptive antenna selection technique. The low-complexity TOSM is capable of improving both the spectrum- and energy-efficiency. In order to further increase the attainable spectrum efficiency, SM was combined with non-orthogonal-multiple-access (NOMA) technique [18]. Furthermore, Zhu *et al.* [9] investigated a NOMA aided SM system, in which successive interference cancellation was adopted by receivers for mitigating the adverse effect of multi-user interference on attainable spectrum efficiency. In contrast to TSM, Zhang *et al.* [10] studied RSM by further considering the pre-coding at the transmitter. In their system, the receiver was capable of directly demodulating information carried by the RF signal received without any other signal processing, if zero-forcing based precoder was adopted. In [19], bit- and symbol-level error probabilities as well as attainable spectrum efficiency of RSM were derived in closed-form expressions.

In order to carefully coordinate both WIT and WPT in RF bands, Hu *el al.* [20] provided a systematic architecture introduction of RF signal based SWIPT, which summarised key enabling techniques of hardware implementation, physical layer, MAC layer and network layer. Specifically, Lv *et al.* [21] studied MIMO based transceiver design for SWIPT, where the optimal power splitting factor for each user is obtained. Wang *et al.* [22] conceived a full-duplex aided relay, which simultaneously received information and harvested energy from RF signals emitted by the source and then forwarded the information to the destination by consuming its energy harvested. Moreover, Zhao *et al.* [23] proposed an enhanced carrier-sensing-multiple-access-collision-avoidance (CSMA/CA) protocol for random access of communication devices powered by RF signal based WPT.

However, the impact of the modulation design on the SWIPT performance has been largely overlooked by the existing literature so far. The basic principle of the SWIPT oriented modulation design has been introduced in [24]. Furthermore, constellation reconfiguration based modulation design was proposed in [25] for the NOMA-SWIPT system. Some initial attempts for SM aided SWIPT system have been made in [13], [26]–[28]. Specifically, Guo *et al.* [13] proposed a TSM

based SWIPT scheme, where one RF chain is equipped at the transmitter. The power splitting factors are determined by maximizing the throughput of the information receiver subject to a certain energy harvesting constraint. Meng *et al.* [26] also studied a TSM-SWIPT system, where they modulated information by the indices of the activated antenna in order to improve the spectrum efficiency, while remaining antennas can be relied upon for energy harvesting. Zhang *et al.* [27] investigated the energy pattern based modulation design for SWIPT by adopting the similar methodology of SM. Furthermore, Cheng *et al.* [28] studied the RSM aided SWIPT system by analysing the attainable rate and the amount of energy harvested. However, they only assumes ideally Gaussian distributed transmit signals, while ignoring the impact of finite alphabets on the SWIPT performance.

### *C. Contributions*

In a RSM aided WIT system, only several receive antennas are activated for modulated symbol reception and demodulation, while the others remain silent. The basic idea of a RSM aided SWIPT system is to activate idle antennas for energy harvesting. However, RF signals received by these idle antennas may interfere the information demodulation. Therefore, we have to carefully design the transceiver of RSM aided SWIPT system in order to achieve optimal SWIPT performance. Our novel contributions are summarised as follows:

- We investigated a *RSM aided SWIPT system* by conceiving three different transmission schemes, which are differentiated from one another by their distinct ways of superimposing dedicated information and energy signals at the transmitter.
- The SWIPT performances in terms of *energy harvested, the bit-error-ratio (BER) and the attainable throughput* are all derived in closed-form by conceiving finite transmit alphabets.
- The *optimal transceiver design of the RSM aided SWIPT system* is obtained for the sake of maximising total amount of energy harvested, while ensuring various WIT requirements.

The rest of our paper is organized as follows: An RSM aided SWIPT system is introduced in Section II, which is followed by the SWIPT performance analysis in Section III. The optimal

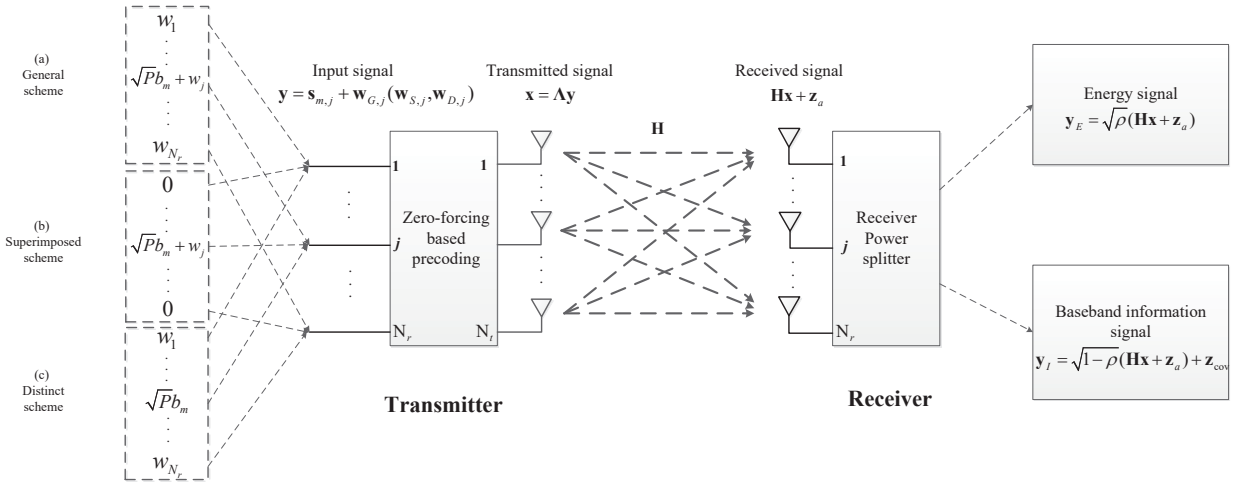


Fig. 1. Three schemes for RSM aided SWIPT, where the information signal is targeted on the $j$-th receive antennas

transceiver is then designed in Section IV, while numerical results are provided in Section V. Finally, our paper is concluded in Section VI.

*Notations:* In this paper, $\mathbb{C}$ denotes the set of complex numbers. $\mathbb{E}[\cdot]$ represents the expectation operation, $\mathcal{R}(\cdot)$ represents the operation of taking the real part of a complex number, while tr$(\cdot)$ represents the trace of a matrix. $|x|$ represents the absolute value of a complex variable $x$, while $\|\mathbf{x}\|_2$ denotes the 2-norm of the vector $\mathbf{x}$. Moreover, $\mathbf{X}^*$ (or $\mathbf{x}^*$) denotes the conjugate transpose of the matrix $\mathbf{X}$ (or the vector $\mathbf{x}$), while $(\mathbf{X})_{i,j}$ represents the entry in the $i$-th row and $j$-th column of the matrix $\mathbf{X}$.

## II. System Model

A MIMO system having a transmitter equipped with $N_t$ antennas and a receiver equipped with $N_r$ antennas is considered, where we have $N_t > N_r$, as shown in Fig. 1. The coefficients of the wireless channel between the transmitter and the receiver are denoted as $\mathbf{H} \in \mathbb{C}^{N_r \times N_t}$, which is unchanged during a symbol duration, while varies between different symbol durations. The classic M-ary PSK/QAM is adopted for modulating information in the conventional amplitude and phase domain. Resultant modulated symbols $\{b_m | m = 1, \cdots, M\}$ have a unity power in average. Therefore, $k_c = \log(M)$ information bits can be transmitted per channel use. Furthermore,

additional information bits can also be modulated in the spatial domain by adopting RSM, since the transmitter may form a beam targeting a specific receive antenna. The index of this targeted receive antenna is also capable of carrying information bits. Therefore, in the spatial domain, $k_s = \log(N_r)$ information bits can be transmitted per channel use. We also assume that information bits '1' and '0' are generated with equal probabilities.

### A. Transmit Signal Model

Without loss of generality, when the $j$-th receive antenna is targeted, the information signal $\mathbf{s}_{m,j}$ received by the receiver can be expressed as

$$\mathbf{s}_{m,j} = [0 \cdots \underbrace{\sqrt{P_s} b_m}_{j\text{-th receive antenna}} \cdots 0]^T, \tag{1}$$

where $P_s$ is the received signal power on the targeted receive antenna. Observe from Eq. (1) that only the $j$-th receive antenna receives the conventionally modulated symbol $b_m$. In order to increase the WPT performance, dedicated energy signals are simultaneously transmitted to the receiver. After the channel attenuation, the received energy signal is denoted as $\mathbf{w} = [w_1, \cdots, w_{N_r}]^T$, whose entries are Gaussian distributed random variables having zero means. The covariance matrix of the received energy signal $\mathbf{w}$ is $\mathbf{\Omega} = \mathbb{E}[\mathbf{w}\mathbf{w}^*]$. Therefore, the $j$-th entry $w_j$ in vector $\mathbf{w}$ has a variance of $(\mathbf{\Omega})_{j,j}$. The received SWIPT signal is then expressed as

$$\mathbf{y} = \mathbf{s}_{m,j} + \mathbf{w}. \tag{2}$$

Moreover, zero-forcing (ZF) precoder [29] is adopted at the transmitter. As a result, the receiver do not need further processing on the received signals, which then reduces the demodulation complexity of the receiver. The resultant ZF precoding matrix $\mathbf{\Lambda}$ is then obtained as

$$\mathbf{\Lambda} = \mathbf{H}^*(\mathbf{H}\mathbf{H}^*)^{-1}. \tag{3}$$

Therefore, the transmit signal is derived as $\mathbf{x} = \mathbf{\Lambda y}$.

### *B. Receive Signal Model*

The receiver is capable of simultaneously harvesting energy and demodulating information by implementing a power splitter. The power splitting ratio is $\rho$. It represents that a portion $\sqrt{\rho}$ of RF signal flows into the energy harvester, while the other portion $\sqrt{1-\rho}$ flows into the information demodulator. Therefore, the actual received RF signal for energy harvesting is expressed as

$$\mathbf{y}_E = \sqrt{\rho}(\mathbf{Hx} + \mathbf{z}_a) = \sqrt{\rho}(\mathbf{H\Lambda y} + \mathbf{z}_a) = \sqrt{\rho}(\mathbf{s}_{m,j} + \mathbf{w} + \mathbf{z}_a), \tag{4}$$

where $\mathbf{z}_a \in \mathbb{C}^{N_r \times 1}$ represents the Additive White Gaussian Noise (AWGN) imposed on the receive antennas. For $\forall j$, its $j$-th entry $z_{a,j} \sim \mathbb{C}\mathcal{N}(0, \sigma_a^2)$ has a zero mean and a variance of $\sigma_a^2/2$ per dimension.

Moreover, the received signal for information demodulation is expressed by

$$\mathbf{y}_I = \sqrt{1-\rho}(\mathbf{H\Lambda y} + \mathbf{z}_a) + \mathbf{z}_{\text{cov}} = \sqrt{1-\rho}(\mathbf{s}_{m,j} + \mathbf{w} + \mathbf{z}_a) + \mathbf{z}_{\text{cov}}, \tag{5}$$

where $\mathbf{z}_{\text{cov}}$ indicates the AWGN imposed by the pass-band to base-band converter. For $\forall j$, its $j$-th entry $z_{\text{cov},j} \sim \mathbb{C}\mathcal{N}(0, \sigma_{\text{cov}}^2)$ has a zero mean and a variance of $\sigma_{\text{cov}}^2/2$ per dimension.

In order to recover the transmit symbol $\mathbf{s}_{m,j}$, a maximum likelihood (ML) detector is adopted for reducing the symbol error rate (SER). The demodulation process can be formulated by

$$(\widehat{j}, \widehat{m}) = \arg \min_{\substack{j' \in [1, N_r] \\ m' \in [1, M]}} (\|\mathbf{y}_I / \sqrt{1-\rho} - \mathbf{s}_{m',j'}\|_2^2), \tag{6}$$

where $\widehat{j}$ is the estimated index of receive antenna and $\widehat{m}$ is the estimated index of the conventionally modulated symbol, while $j'$ is the trial index of receive antenna and $m'$ is the trial index of the conventionally modulated symbol in the hypothesis-detection problem.

### C. Transmission Schemes

Since we superimpose the dedicated energy signals $\mathbf{w}$ onto the information signal $\mathbf{s}_{m,j}$, as expressed in Eq. (2), the SER performance at the receiver is inevitably degraded. The dedicated energy signal on different receive antennas may affect the demodulation in both the spatial and the conventional domains. For instance, if the conventionally modulated symbol is transmitted by targeting the $j$-th receive antenna, the energy signal on the $j$-th receive antenna may interfere the demodulation in the conventional domain. Moreover, the energy signals received by other antennas may mislead the demodulation in the spatial domain, since the power of the dedicated energy signals make the demodulator hard to identify the index of the receive antenna originally targeted by the transmitter. Therefore, we consider the following three transmission schemes for superimposing dedicated energy signals on information signals at the transmitter of the RSM aided SWIPT system:

- **General scheme,** as exemplified in Fig. 1 (a), allows the dedicated energy signals transmitted by targeting all the receive antennas. For example, if the $j$-th receive antenna is targeted for receiving the conventionally modulated symbol, the actual received signal on the $j$-th antenna is a superposition of the dedicated energy signal and the conventionally modulated information signal. By contrast, on other antennas, only dedicated energy signals are received. The dedicated energy signals in this scheme is obtained as $\mathbf{w}_{G,j} = \mathbf{w}$, where $\mathbf{w}$ has been defined in Section II-A.
- **Superimposed scheme,** as illustrated in Fig. 1 (b), only superimposes the dedicated energy signal on the conventionally modulated symbol, which targets for the $j$-th antenna. Therefore, the dedicated energy signal in this scheme is expressed as $\mathbf{w}_{S,j} = \mathbf{A}_{S,j}\mathbf{w}$, where $\mathbf{A}_{S,j}$ is a $N_r \times N_r$ matrix having its entry in $j$-th row and $j$-th column equal to a unity but all the other entries equal to zero. As a result, the dedicated energy signal only interferes the demodulation in the conventional domain.
- **Distinct scheme,** as illustrated in Fig. 1 (c), allows the dedicated energy signals to target

all the receive antennas except the $j$-th one, if the conventionally modulated symbol targets the $j$-th receive antenna. The dedicated energy signal is then expressed as $\mathbf{w}_{D,j} = \mathbf{A}_{D,j}\mathbf{w}$, where $\mathbf{A}_{D,j}$ is a $N_r \times N_r$ matrix having its entry in the $j$-th row and $j$-th column equal to zero but all the others equal to a unity.

Intuitively, the general scheme has best WPT performance, since full degree of freedom in the spatial domain is exploited for transmitting dedicated energy signal. By contrast, the superimposed scheme and the distinct scheme may have lower SER performance, since the dedicated energy signal may only interfere the demodulation in either the conventional or the spatial domain.

## III. Performance Analysis of RSM aided SWIPT

### A. WPT Performance Analysis

Without loss of generality, we represent the dedicated energy signal by the vector $\mathbf{w}$. Therefore, the average energy harvested by the receiver for a single symbol duration is calculated as

$$\begin{aligned}
E &= \xi T \mathbb{E}\left[\|\mathbf{y}_E\|_2^2\right] \\
&= \xi T\rho \frac{1}{M}\frac{1}{N_r}\sum_{m=1}^{M}\sum_{j=1}^{N_r}\mathbb{E}\left[\|\mathbf{s}_{m,j}+\mathbf{w}\|_2^2\right] + \xi T\rho\mathbb{E}\left[\|\mathbf{z}_a\|_2^2\right] \\
&= \xi T\rho \frac{1}{M}\frac{1}{N_r}\sum_{m=1}^{M}\sum_{j=1}^{N_r}\mathbb{E}\left[\sum_{i=1,i\neq j}^{N_r}|w_i|^2 + (\sqrt{P_s}b_m + w_j)(\sqrt{P_s}b_m^* + w_j^*)\right] + \xi T\rho N_r\sigma_a^2 \\
&= \xi T\rho \frac{1}{M}\frac{1}{N_r}\sum_{m=1}^{M}\sum_{j=1}^{N_r}\mathbb{E}\left[\sum_{i=1}^{N_r}|w_i|^2 + P_s|b_m|^2 + 2\mathcal{R}(\sqrt{P_s}b_m^* w_j)\right] + \xi T\rho N_r\sigma_a^2 \\
&= \xi T\rho(P_s + \mathrm{Tr}(\mathbf{\Omega}) + N_r\sigma_a^2), \qquad (7)
\end{aligned}$$

where $T$ represents the transmitting duration for a single symbol, $\xi \in [0, 1]$ represents the energy harvesting efficiency.

For the *General Scheme* of Section II-C, the amount of energy harvested $E_G$ can be calculated by Eq. (7), since we have $\mathbf{w}_{G,j} = \mathbf{w}$.

For the *Superimposed Scheme*, we substitute w by $\mathbf{w}_{S,j} = \mathbf{A}_{S,j}\mathbf{w}$ in the fourth line of (7). The corresponding energy harvesting performance is derived as

$$\begin{aligned} E_S &= \xi T\rho \frac{1}{M}\frac{1}{N_r}\sum_{m=1}^{M}\sum_{j=1}^{N_r}\mathbb{E}\left[\|\mathbf{s}_{m,j}+\mathbf{w}_{S,j}\|_2^2\right] + \xi T\rho\mathbb{E}\left[\|\mathbf{z}_a\|_2^2\right] \\ &= \xi T\rho(P_s + \mathrm{Tr}(\mathbf{\Omega})/N_r + N_r\sigma_a^2). \end{aligned} \tag{8}$$

Finally, By substituting $\mathbf{w}_{D,j} = \mathbf{A}_{D,j}\mathbf{w}$ into Eq. (7), the energy harvesting performance of the *Distinct Scheme* can be expressed as

$$\begin{aligned} E_D &= \xi T\rho \frac{1}{M}\frac{1}{N_r}\sum_{m=1}^{M}\sum_{j=1}^{N_r}\mathbb{E}\left[\|\mathbf{s}_{m,j}+\mathbf{w}_{D,j}\|_2^2\right] + \xi T\rho\mathbb{E}\left[\|\mathbf{z}_a\|_2^2\right] \\ &= \xi T\rho(P_s + (N_r-1)\mathrm{Tr}(\mathbf{\Omega})/N_r + N_r\sigma_a^2). \end{aligned} \tag{9}$$

### *B. BER Performance Analysis*

Regardless of any specific transmission scheme, we still use $\mathbf{w}$ to represent the dedicated energy signal. The alphabetical set of the modulated symbols is denoted as $\mathcal{S} = \{\mathbf{s}_{m,j} | j \in [1, N_r], m \in [1, M]\}$, whose cardinality is $|\mathcal{S}| = MN_r$. The union-bound approach [10] is then exploited for deriving the upper-bound of the BER $\epsilon$ of the RSM aided SWIPT, when the ML detector is adopted. The upper-bound of the BER $\epsilon$ is then expressed as

$$\epsilon = \frac{1}{k|\mathcal{S}|}\sum_{\mathbf{s}_{m,j}\in\mathcal{S}}\sum_{\mathbf{s}_{n,i}\in\mathcal{S}\neq\mathbf{s}_{m,j}} d(\mathbf{s}_{m,j}, \mathbf{s}_{n,i})\tau(\mathbf{s}_{m,j} \to \mathbf{s}_{n,i}), \tag{10}$$

where $k = k_s + k_c$ is the total number of bits carried by a modulated symbol in both the spatial and conventional domains, $d(\mathbf{s}_{m,j}, \mathbf{s}_{n,i})$ represents the Hamming distance between the information bits carried by the symbol $\mathbf{s}_{m,j}$ and those carried by the symbol $\mathbf{s}_{n,i}$, whereas $\tau(\mathbf{s}_{m,j} \to \mathbf{s}_{n,i})$ represents the pairwise error probability (PEP) that the transmit symbol $\mathbf{s}_{m,j}$ is demodulated as $\mathbf{s}_{n,i}$.

*1) PEP derivation:* There are three cases of $\tau(\mathbf{s}_{m,j} \to \mathbf{s}_{n,i})$, which is formulated as

$$\tau(\mathbf{s}_{m,j} \to \mathbf{s}_{n,i}) = \begin{cases} \tau_S(\mathbf{s}_{m,j} \to \mathbf{s}_{m,i}), i \neq j, m = n, \\ \tau_C(\mathbf{s}_{m,j} \to \mathbf{s}_{n,j}), i = j, m \neq n, \\ \tau_B(\mathbf{s}_{m,j} \to \mathbf{s}_{n,i}), i \neq j, m \neq n. \end{cases} \tag{11}$$

In Eq. (11), $\tau_S(\mathbf{s}_{m,j} \to \mathbf{s}_{m,i})$ represents the probability of the demodulation error only occurring in the spatial domain and $\tau_C(\mathbf{s}_{m,j} \to \mathbf{s}_{n,j})$ is the probability of the demodulation error only occurring in the conventional domain, while $\tau_B(\mathbf{s}_{m,j} \to \mathbf{s}_{n,i})$ is the probability of the demodulation error occurring in both spatial and conventional domains. The following theorems are then proposed for deriving these three probabilities.

*Theorem 1:* The probability of the original transmit symbol $\mathbf{s}_{m,j}$ being demodulated as $\mathbf{s}_{m,i}$, the probability of the original transmit symbol $\mathbf{s}_{m,j}$ being demodulated as $\mathbf{s}_{n,j}$ as well as the probability of the original transmit symbol $\mathbf{s}_{m,j}$ being demodulated as $\mathbf{s}_{n,i}$ are formulated as:

$$\begin{aligned} \tau_S(\mathbf{s}_{m,j} \to \mathbf{s}_{m,i}) &= Q\left(\frac{\sqrt{P_s}|b_m|}{\sqrt{(\mathbf{\Omega})_{i,i}/2 + (\mathbf{\Omega})_{j,j}/2 + \sigma_a^2 + \sigma_{\text{cov}}^2/(1-\rho)}}\right), \\ \tau_C(\mathbf{s}_{m,j} \to \mathbf{s}_{n,j}) &= Q\left(\frac{\sqrt{P_s}(|b_n|^2 + |b_m|^2)/2 - \mathcal{R}(b_m^* b_n)}{|b_n - b_m|\sqrt{(\mathbf{\Omega})_{j,j}/2 + \sigma_a^2/2 + \sigma_{\text{cov}}^2/2(1-\rho)}}\right), \\ \tau_B(\mathbf{s}_{m,j} \to \mathbf{s}_{n,i}) &= Q\left(\frac{\sqrt{P_s}(|b_n|^2 + |b_m|^2)/2}{\sqrt{|b_n|^2(\mathbf{\Omega})_{i,i}/2 + |b_m|^2(\mathbf{\Omega})_{j,j}/2 + (|b_n|^2 + |b_m|^2)(\sigma_a^2/2 + \sigma_{\text{cov}}^2/2(1-\rho))}}\right). \end{aligned} \tag{12}$$

*Proof:* Please refer to Appendix A for detailed proof. ■

*2) BER derivation:* The upper-bound of the corresponding BER can be then derived as

$$\begin{aligned} \epsilon = \frac{1}{kMN_r} \sum_{\mathbf{s}_{m,j} \in \mathcal{S}} \Bigg( & \sum_{\substack{\mathbf{s}_{m,i} \in \mathcal{S} \\ i \neq j}} d(\mathbf{s}_{m,j}, \mathbf{s}_{m,i}) \tau_S(\mathbf{s}_{m,j} \to \mathbf{s}_{m,i}) \\ & + \sum_{\substack{\mathbf{s}_{n,j} \in \mathcal{S} \\ n \neq m}} d(\mathbf{s}_{m,j}, \mathbf{s}_{n,j}) \tau_C(\mathbf{s}_{m,j} \to \mathbf{s}_{n,j}) + \sum_{\substack{\mathbf{s}_{n,i} \in \mathcal{S} \\ i \neq j, n \neq m}} d(\mathbf{s}_{m,j}, \mathbf{s}_{n,i}) \tau_B(\mathbf{s}_{m,j} \to \mathbf{s}_{n,i}) \Bigg). \end{aligned} \tag{13}$$

For the *General Scheme*, we have $\mathbf{w}_{G,j} = \mathbf{w}$. Its corresponding covariance matrix is formulated

as $\mathbf{\Omega}_{G,j} = \mathbf{\Omega}$. Therefore, its corresponding PEP $\tau_S^G$, $\tau_C^G$, $\tau_B^G$ can be calculated by Eq. (12), respectively. By substituting these PEPs to (13), the BER $\epsilon_G$ of the *General Scheme* can be derived.

For the *Superimposed Scheme*, we have $\mathbf{w}_{S,j} = \mathbf{A}_{S,j}\mathbf{w}$, since the information targets the $j$-th receive antenna. Its corresponding covariance matrix is formulated as $\mathbf{\Omega}_{S,j} = \mathbf{A}_{S,j}\mathbf{\Omega}\mathbf{A}_{S,j}^*$, which satisfies $(\mathbf{\Omega}_{S,j})_{i,i} = (\mathbf{\Omega})_{j,j} \cdot Ind(i = j)$, where $Ind(x)$ is a indicator function satisfying $Ind(x) = 1$, if the boolean parameter $x$ is true, and $Ind(x) = 0$, otherwise. By substituting $\mathbf{\Omega}_{S,j}$ to Eq. (12), respectively, the PEPs of the *Superimposed Scheme* are formulated as

$$\begin{aligned}
\tau_S^S(\mathbf{s}_{m,j} \to \mathbf{s}_{m,i}) &= Q\left(\frac{\sqrt{P_s}|b_m|}{\sqrt{(\mathbf{\Omega})_{j,j}/2 + \sigma_a^2 + \sigma_{\text{cov}}^2/(1-\rho)}}\right), \\
\tau_C^S(\mathbf{s}_{m,j} \to \mathbf{s}_{n,j}) &= Q\left(\frac{\sqrt{P_s}(|b_n|^2 + |b_m|^2)/2 - \mathcal{R}(b_m^* b_n)}{|b_n - b_m|\sqrt{(\mathbf{\Omega})_{j,j}/2 + \sigma_a^2/2 + \sigma_{\text{cov}}^2/2(1-\rho)}}\right), \\
\tau_B^S(\mathbf{s}_{m,j} \to \mathbf{s}_{n,i}) &= Q\left(\frac{\sqrt{P_s}(|b_n|^2 + |b_m|^2)/2}{\sqrt{|b_m|^2(\mathbf{\Omega})_{j,j}/2 + (|b_n|^2 + |b_m|^2)(\sigma_a^2/2 + \sigma_{\text{cov}}^2/2(1-\rho))}}\right),
\end{aligned} \tag{14}$$

respectively. The upper-bounded BER $\epsilon_S$ can be further derived by substituting $\tau_S^S$, $\tau_C^S$ and $\tau_B^S$ to Eq. (13).

For the *Distinct scheme*, we have $\mathbf{w}_{D,j} = \mathbf{A}_{D,j}\mathbf{w}$. Its corresponding covariance matrix is $\mathbf{\Omega}_{D,j} = \mathbf{A}_{D,j}\mathbf{\Omega}\mathbf{A}_{D,j}^*$, whose element in the $i$-th row and the $i$-th column satisfies $(\mathbf{\Omega}_{D,j})_{i,i} = (\mathbf{\Omega})_{j,j} \cdot (1 - Ind(i = j))$. By substituting $\mathbf{\Omega}_{D,j}$ to Eq. (12), the PEPs of the *Distinct Scheme* are formulated as

$$\begin{aligned}
\tau_S^D(\mathbf{s}_{m,j} \to \mathbf{s}_{m,i}) &= Q\left(\frac{\sqrt{P_s}|b_m|}{\sqrt{(\mathbf{\Omega})_{i,i}/2 + \sigma_a^2/2 + \sigma_{\text{cov}}^2/(1-\rho)}}\right), \\
\tau_C^D(\mathbf{s}_{m,j} \to \mathbf{s}_{n,j}) &= Q\left(\frac{\sqrt{P_s}(|b_n|^2 + |b_m|^2)/2 - \mathcal{R}(b_m^* b_n)}{|b_n - b_m|\sqrt{\sigma_a^2/2 + \sigma_{\text{cov}}^2/2(1-\rho)}}\right), \\
\tau_B^D(\mathbf{s}_{m,j} \to \mathbf{s}_{n,i}) &= Q\left(\frac{\sqrt{P_s}(|b_n|^2 + |b_m|^2)/2}{\sqrt{|b_n|^2(\mathbf{\Omega})_{i,i}/2 + (|b_n|^2 + |b_m|^2)(\sigma_a^2/2 + \sigma_{\text{cov}}^2/2(1-\rho))}}\right).
\end{aligned} \tag{15}$$

The upper-bounded BER $\epsilon_D$ of the *Distinct Scheme* can be further derived by substituting $\tau_S^D$, $\tau_C^D$ and $\tau_B^D$ to Eq. (13).

### C. Throughput performance analysis

The information transmission between the transmitter and the receiver can be modelled as a memoryless binary symmetric channel (BSC). The crossover probability of the BSC is the BER derived in Section III-B. Therefore, the mutual information $I(x;\widehat{y})$ of the RSM aided SWIPT system between the input bit $x \in \{0,1\}$ and the estimated output bit $\widehat{y} \in \{0,1\}$ is formulated as

$$I(x;\widehat{y}) = H(\widehat{y}) - H(\widehat{y}|x), \tag{16}$$

where $H(\cdot)$ is the entropy function. Given the generation probability $p_{x0}$ of bit 0 and that $p_{x1}$ of bit 1, $H(\widehat{y})$ is expressed as

$$\begin{aligned} H(\widehat{y}) =& - p_{\widehat{y}0}\log(p_{\widehat{y}0}) - p_{\widehat{y}1}\log(p_{\widehat{y}1}) \\ =& - (p_{x0}p_{\widehat{y}0|x0} + p_{x1}p_{\widehat{y}0|x1})\log(p_{x0}p_{\widehat{y}0|x0} + p_{x1}p_{\widehat{y}0|x1}) \\ & - (p_{x0}p_{\widehat{y}1|x0} + p_{x1}p_{\widehat{y}1|x1})\log((p_{x0}p_{\widehat{y}1|x0} + p_{x1}p_{\widehat{y}1|x1})), \end{aligned} \tag{17}$$

where $p_{\widehat{y}j}$ is the probability of the estimated output bit being $\widehat{y} = j$ for $j \in \{0,1\}$, $p_{\widehat{y}j|xi}$ is the probability that the input bit $x = i$ is decoded as the estimated output bit $\widehat{y} = j$. In the BSC, we have $p_{\widehat{y}0|x1} = p_{\widehat{y}1|x0} = \epsilon$, where $\epsilon$ is either $\epsilon_G$, $\epsilon_S$ or $\epsilon_D$, when the corresponding transmission scheme is adopted. Then, $H(\widehat{y})$ of Eq. (17) can be reformulated as

$$H(\widehat{y}) = -(p_{x0}(1-\epsilon) + p_{x1}\epsilon)\log(p_{x0}(1-\epsilon) + p_{x1}\epsilon) - (p_{x1}(1-\epsilon) + p_{x0}\epsilon)\log(p_{x1}(1-\epsilon) + p_{x0}\epsilon). \tag{18}$$

By substituting $p_{x0} = p_{x1} = 0.5$ into (18), the entropy of the channel output is $H(\widehat{y}) = 1$. In this case, the noise entropy $H(\widehat{y}|x)$ is derived as

$$H(\widehat{y}|x) = -\sum_{i\in\{0,1\}} p_{xi} \sum_{j\in\{0,1\}} p_{\widehat{y}j|xi}\log(p_{\widehat{y}j|xi}) = -\epsilon\log\epsilon - (1-\epsilon)\log(1-\epsilon). \tag{19}$$

Finally, the achievable rate during each transmission becomes

$$R = kI(x;\widehat{y}) = k(1 + \epsilon \log \epsilon + (1-\epsilon)\log(1-\epsilon)), \tag{20}$$

where $k$ is the number of bits carried by a modulated symbol in the RSM aided SWIPT system.

By substituting $\epsilon$ in (20) by $\epsilon_G$, $\epsilon_S$ and $\epsilon_D$, respectively, the achievable rate $R_G$, $R_S$ and $R_D$ of all three transmission schemes can be derived accordingly.

## IV. Transceiver Design of RSM aided SWIPT

### A. Problem Formulation

The transmit power at the transmitter is calculated as:

$$\begin{aligned} P_t =& \mathbb{E}[\mathrm{tr}(\mathbf{x}\mathbf{x}^*)] \\ =& 1/N_r P_s \mathrm{tr}(\mathbf{\Lambda}\mathbf{\Lambda}^*) + \mathrm{tr}(\mathbf{\Lambda}\mathbf{\Omega}\mathbf{\Lambda}^*), \end{aligned} \tag{21}$$

which is also the transmit power for the *General Scheme*. For the *Superimposed Scheme* and the *Distinct Scheme*, the term "$\mathrm{tr}(\mathbf{\Lambda}\mathbf{\Omega}\mathbf{\Lambda}^*)$" of (21) is substituted by $\frac{\mathrm{tr}(\mathbf{\Lambda}\mathbf{\Omega}\mathbf{\Lambda}^*)}{N_r}$ and $\frac{(N_r-1)\mathrm{tr}(\mathbf{\Lambda}\mathbf{\Omega}\mathbf{\Lambda}^*)}{N_r}$, respectively.

A general optimal transceiver design for all these three transmission schemes is formulated as

$$\text{(P1)} \quad \max_{P_s,\mathbf{\Omega},\rho} E \tag{22}$$

$$\text{s.t.} \quad \epsilon \le \epsilon_{\mathrm{th}}, \tag{22a}$$

$$R \ge R_{\mathrm{th}}, \tag{22b}$$

$$P_t \le P_{\max}. \tag{22c}$$

(P1) aims for maximising the energy harvested at the receiver by finding the optimal signal power $P_s$ of the modulated information signal, covariance matrix $\mathbf{\Omega}$ of the dedicated energy

signal as well as the power splitting ratio $\rho$ at the receiver, while ensuring that the BER upper bound $\epsilon$ should be lower than a specific threshold $\epsilon_{\text{th}}$, as expressed in (22a), and the achievable rate $R$ should be higher than a specific threshold $R_{\text{th}}$, as expressed in (22b). Furthermore, the transmit power $P_t$ is not allowed to exceed $P_{\max}$, as expressed in (22c).

According to (20), the information rate $R$ of the RSM aided SWIPT system is always a monotonously decreasing function with respect to the BER $\epsilon$. Therefore, the constraints (22a) and (22b) can be substituted by a single constraint of $\epsilon \leq \epsilon'_{\text{th}}$, where $\epsilon'_{\text{th}}$ is carefully chosen for simultaneously satisfying the original rate and BER constraints. The original problem (P1) is then reformulated as

$$\text{(P2)} \quad \max_{P_s, \mathbf{\Omega}, \rho} E \tag{23}$$

$$\text{s.t.} \quad \epsilon \leq \epsilon_{\text{th}}^{'}, \tag{23a}$$

$$P_t \leq P_{\max}. \tag{23b}$$

### *B. Characteristics of Dedicated Energy Signal*

By exploring the characteristics of the dedicated energy signal, we may substantially reduce the number of variables to be optimised. Since dedicated energy signals targeting for different receive antennas are independent of each other, we have $(\mathbf{\Omega})_{i,j} = 0$ for $i \neq j$ in the covariance matrix $\mathbf{\Omega}$. Therefore, $\mathbf{\Omega}$ only has $N_r$ non-zero elements in its diagonal.

*Remark 1:* The BER upper-bounds $\epsilon_G, \epsilon_S, \epsilon_D$ are all monotonically decreasing functions with respect to (w.r.t.) the signal power $P_s$. They are also monotonically increasing functions w.r.t. the power slitting ratio $\rho$ and all the diagonal elements of the covariance matrix $\mathbf{\Omega}$. So are the energy harvesting performance $E_G, E_S$ and $E_D$.

Let $\mathbf{\Lambda}_j$ for $j = 1, \cdots, N_r$ represents the $j$-th column of the transmit precoding matrix $\mathbf{\Lambda}$, the following theorem provides the main characteristics of the covariance matrix of the dedicated energy signal:

*Theorem 2:* When a solution to (P2) is optimal, the energy signal must satisfy $(\mathbf{\Omega})_{j,j} = 0$, if we have $\|\mathbf{\Lambda}_j\|_2^2 \geq \frac{1}{N_r}\sum_{i=1}^{N_r}\|\mathbf{\Lambda}_i\|_2^2$ for $j = 1, \cdots, N_r$. This theorem is valid for all the three transmission schemes of Section II-C.

*Proof:* Please refer to Appendix B for detailed proof. ■

## C. Convex Transformation

Although the function $Q(x)$ is concave w.r.t. $x$, the upper bound BER $\epsilon$ is not convex w.r.t. $P_s$ and $\mathbf{\Omega}$. Therefore, we aim for transforming the non-convex (P2) to a convex optimisation problem. According to Eq. (13), the BER upper bound $\epsilon$ consists of three parts, namely $\tau_S$, $\tau_C$ and $\tau_B$. Therefore, (P2) can be reformulated as

$$\text{(P3)} \quad \max_{P_s, \mathbf{\Omega}, \rho} E \tag{24}$$

$$\text{s.t.} \quad \tau_S(\mathbf{s}_{m,j} \to \mathbf{s}_{m,i}) \leq \epsilon_0, \forall i \neq j \in [1, N_r], m \in [1, M], \tag{24a}$$

$$\tau_C(\mathbf{s}_{m,j} \to \mathbf{s}_{n,j}) \leq \epsilon_0, \forall j \in [1, N_r], m \neq n \in [1, M], \tag{24b}$$

$$\tau_B(\mathbf{s}_{m,j} \to \mathbf{s}_{n,i}) \leq \epsilon_0, \forall i \neq j \in [1, N_r], m \neq n \in [1, M], \tag{24c}$$

$$P_t \leq P_{\max}. \tag{24d}$$

The corresponding upper bound BER of (P3) has to satisfy the following inequality:

$$\begin{aligned} \epsilon =& \frac{1}{kMN_r}\sum_{\mathbf{s}_{m,j}\in\mathcal{S}}\sum_{\substack{\mathbf{s}_{n,i}\in\mathcal{S} \\ \mathbf{s}_{n,i}\neq\mathbf{s}_{m,j}}} d(\mathbf{s}_{m,j}, \mathbf{s}_{n,i})\tau(\mathbf{s}_{m,j} \to \mathbf{s}_{n,i}), \\ \leq& \frac{1}{kMN_r}\sum_{\mathbf{s}_{m,j}\in\mathcal{S}}\sum_{\substack{\mathbf{s}_{n,i}\in\mathcal{S} \\ \mathbf{s}_{n,i}\neq\mathbf{s}_{m,j}}} d(\mathbf{s}_{m,j}, \mathbf{s}_{n,i})\epsilon_0 \leq \epsilon_{\text{th}}^{'}, \end{aligned} \tag{25}$$

where the first inequality is derived by considering the constraints (24a)-(24c). The second inequality of Eq. (25) guarantees that the solution to (P3) also satisfy the BER constraint (23a)

of (P2), if we have

$$\epsilon_0 = \frac{kMN_r\epsilon_{\text{th}}^{'}}{\sum\limits_{\mathbf{s}_{m,j}\in\mathcal{S}}\sum\limits_{\substack{\mathbf{s}_{n,i}\in\mathcal{S}\\ \mathbf{s}_{n,i}\neq\mathbf{s}_{m,j}}} d(\mathbf{s}_{m,j},\mathbf{s}_{n,i})}. \tag{26}$$

Since constraints (24a)-(24c) of (P3) constitute a sufficient condition of the constraint (23a) of (P2), the optimal solution to (P3) is a lower-bound of that to (P2).

Moreover, according to *Theorem. 1*, (P3) can be further reformulated as

$$\text{(P4)} \quad \max_{P_s,\mathbf{\Omega},\rho} E \tag{27}$$

$$\text{s.t.} \quad \frac{P_s|b_m|^2}{(\mathbf{\Omega})_{i,i}/2 + (\mathbf{\Omega})_{j,j}/2 + \sigma_a^2 + \sigma_{\text{cov}}^2/(1-\rho)} \geq (Q^{-1}(\epsilon_0))^2, \forall i \neq j \in [1,N_r], m \in [1,M] \tag{27a}$$

$$\frac{P_s\left((|b_n|^2 + |b_m|^2)/2 - \mathcal{R}(b_m^* b_n)\right)^2}{|b_n - b_m|^2\left((\mathbf{\Omega})_{j,j}/2 + \sigma_a^2/2 + \sigma_{\text{cov}}^2/2(1-\rho)\right)} \geq (Q^{-1}(\epsilon_0))^2, \forall j \in [1,N_r], m \neq n \in [1,M] \tag{27b}$$

$$\frac{P_s\left((|b_n|^2 + |b_m|^2)/2\right)^2}{|b_n|^2(\mathbf{\Omega})_{i,i}/2 + |b_m|^2(\mathbf{\Omega})_{j,j}/2 + (|b_n|^2 + |b_m|^2)(\sigma_a^2/2 + \sigma_{\text{cov}}^2/2(1-\rho))} \geq (Q^{-1}(\epsilon_0))^2,$$

$$\forall i \neq j \in [1,N_r], m \neq n \in [1,M] \tag{27c}$$

$$P_t \leq P_{\max}, \tag{27d}$$

where $Q^{-1}(\cdot)$ is the inverse function of $Q(\cdot)$ and $\mathbf{\Omega}$ can be replaced by $\mathbf{\Omega}_{G,j}$, $\mathbf{\Omega}_{S,j}$ or $\mathbf{\Omega}_{D,j}$, respectively, for characterising the corresponding transmission schemes.

Unfortunately, (P4) is still non-convex, since $P_s$, $\mathbf{\Omega}$ and $\rho$ are coupled with one another. Based on Eq. (21), the transmit power can be further expressed as

$$P_t = \sum_{j=1}^{N_r} ||\mathbf{\Lambda}_j||_2^2\left(\frac{P_s}{N_r} + (\mathbf{\Omega})_{j,j}\right). \tag{28}$$

Moreover, based on Eq. (7), the energy harvested by the receiver is reformulated as

$$E = \xi T\rho(P_s + \sum_{j=1}^{N_r}(\mathbf{\Omega})_{j,j} + N_r\sigma_a^2). \tag{29}$$

Since maximising the amount of energy harvested is the same as maximising its logarithm function, by defining $\mu = \frac{1}{1-\rho}$, (P4) can be further equivalently transformed as

$$\text{(P5)} \quad \max_{P_s,\{(\mathbf{\Omega})_{j,j}\},\mu} \log(E) = \log(\xi T) + \log(\frac{\mu-1}{\mu}) + \log(P_s + \sum_{j=1}^{N_r}(\mathbf{\Omega})_{j,j} + N_r\sigma_a^2) \tag{30}$$

$$\text{s.t.} \quad P_s \geq \alpha_{m,0}^S + \alpha_{m,1}^S(\mathbf{\Omega})_{i,i} + \alpha_{m,2}^S(\mathbf{\Omega})_{j,j} + \alpha_{m,3}^S\mu, \forall i \neq j \in [1, N_r], m \in [1, M] \tag{30a}$$

$$P_s \geq \alpha_{m,n,0}^C + \alpha_{m,n,2}^C(\mathbf{\Omega})_{j,j} + \alpha_{m,n,3}^C\mu, \forall j \in [1, N_r], m \neq n \in [1, M] \tag{30b}$$

$$P_s \geq \alpha_{m,n,0}^B + \alpha_{m,n,1}^B(\mathbf{\Omega})_{i,i} + \alpha_{m,n,2}^B(\mathbf{\Omega})_{j,j} + \alpha_{m,n,3}^B\mu, \forall i \neq j \in [1, N_r], m \neq n \in [1, M] \tag{30c}$$

$$\sum_{j=1}^{N_r} \|\mathbf{\Lambda}_j\|^2 \left(\frac{P_s}{N_r} + (\mathbf{\Omega})_{j,j}\right) \leq P_{\max}, \tag{30d}$$

where we have

$$\begin{cases} \alpha_{m,0}^S = \frac{(Q^{-1}(\epsilon_0))^2\sigma_a^2}{|b_m|^2}, \alpha_{m,1}^S = \alpha_{m,2}^S = \frac{(Q^{-1}(\epsilon_0))^2}{2|b_m|^2}, \alpha_{m,3}^S = \frac{(Q^{-1}(\epsilon_0))^2\sigma_{\text{cov}}^2}{|b_m|^2}, \\ \alpha_{m,n,0}^C = \frac{(Q^{-1}(\epsilon_0))^2|b_n-b_m|^2\sigma_a^2}{2\left((|b_n|^2+|b_m|^2)/2-\mathcal{R}(b_m^*b_n)\right)^2}, \alpha_{m,n,2}^C = \frac{(Q^{-1}(\epsilon_0))^2|b_n-b_m|^2}{2\left((|b_n|^2+|b_m|^2)/2-\mathcal{R}(b_m^*b_n)\right)^2}, \\ \alpha_{m,n,3}^C = \frac{(Q^{-1}(\epsilon_0))^2|b_n-b_m|^2\sigma_{\text{cov}}^2}{2\left((|b_n|^2+|b_m|^2)/2-\mathcal{R}(b_m^*b_n)\right)^2}, \alpha_{m,n,0}^B = \frac{2(Q^{-1}(\epsilon_0))^2\sigma_a^2}{\left((|b_n|^2+|b_m|^2)/2\right)}, \alpha_{m,n,1}^B = \frac{(Q^{-1}(\epsilon_0))^2|b_n|^2}{2\left((|b_n|^2+|b_m|^2)/2\right)^2}, \\ \alpha_{m,n,2}^B = \frac{(Q^{-1}(\epsilon_0))^2|b_m|^2}{2\left((|b_n|^2+|b_m|^2)/2\right)^2}, \alpha_{m,n,3}^B = \frac{2(Q^{-1}(\epsilon_0))^2\sigma_{\text{cov}}^2}{\left((|b_n|^2+|b_m|^2)/2\right)}. \end{cases} \tag{31}$$

*Theorem 3:* (P5) is concave w.r.t. $P_s$,$\{(\mathbf{\Omega})_{j,j}|j = 1, \cdots, N_r\}$ and $\mu$.

*Proof:* Please refer to Appendix C for detailed proof. ■

Therefore, the concave optimisation problem (P5) can be efficiently solved by exploiting the convex optimisation tools, such as CVX [30].

## V. Numerical Results

The performance of the RSM aided SWIPT system are then evaluated by both theoretical analysis and Monte-Carlo simulation. We consider $N_t = 8$ antennas for the transmitter and $N_r = \{2, 4, 8\}$ antennas for the receiver. The classic QPSK, 8PSK and 16QAM are adopted as the conventional modulator. The channel coefficient $\mathbf{H}$ between the transmitter and the receiver is

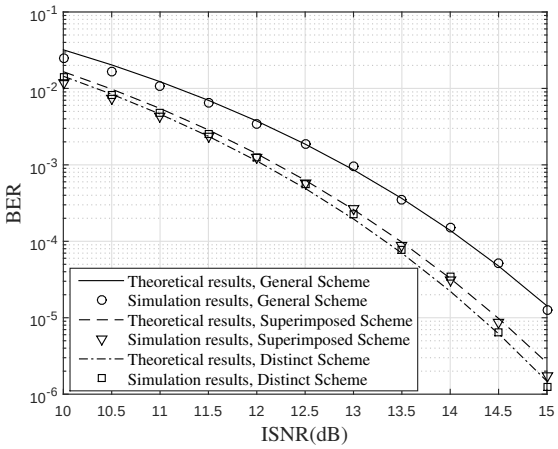


Fig. 2. Validation of theoretical analysis, when QPSK is adopted in the conventional domain and $N_r = 2$.

expressed as $\mathbf{H} = \mathbf{C}d^{-\beta}$ where $d = 10$ m is the distance between the transmitter and the receiver and $\beta = 3$ is the path-loss exponent, $\mathbf{C} \in \mathbb{C}^{N_t \times N_r}$ represents the multipath Rayleigh fading having a unity mean. The noise power is $\sigma_a^2 = \sigma_{\text{cov}}^2 = -60$ dBm.

### A. Validation of Theoretical Analysis

We first validate our theoretical BER analysis in Fig. 2, where the variances of the dedicated energy signal are set to $(\mathbf{\Omega})_{1,1} = \cdots = (\mathbf{\Omega})_{N_r,N_r} = -20$dBm and the power splitting ratio is set to $\rho = 0.99$. The information-signal-to-noise-ratio (ISNR) in the x-coordinate is given as $\text{ISNR} = P_s(1-\rho)/((1-\rho)\sigma_a^2 + \sigma_{\text{cov}}^2)$. Observe from Fig. 2 that the theoretical upper bound of the BER is almost the same as the actual BER of the Monte-Carlo simulation. Since the gap between theoretical and simulation results is negligible, we choose to use our theoretical analysis to evaluate the system performance, while abandoning the time-consuming Monte-Carlo simulation based performance evaluation. Furthermore, we also observe from Fig. 2 that the *Distinct Scheme* outperforms the other counterparts in terms of the BER.

### B. SWIPT Performance

With the same parameter settings as Fig. 2, we evaluate the BER performance by adopting different conventional modulators as well as different number of receive antennas in Fig. 3.

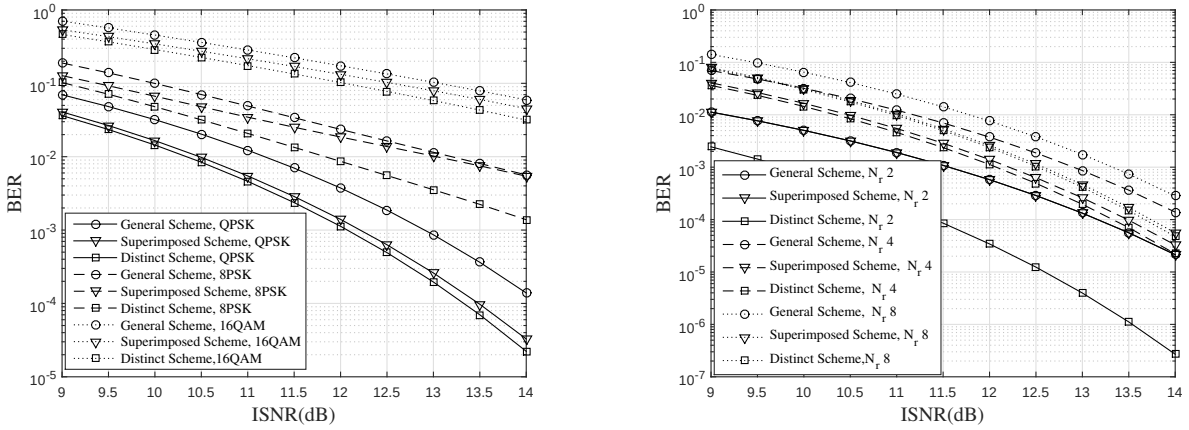


(a) BER versus ISNR with different modulator, where $N_r = 4$

(b) BER versus ISNR with different number of receive antennas number using QPSK

Fig. 3. BER versus ISNR of the RSM-SWIPT system

Observe from Fig. 3 that the *Distinct Scheme* has the lowest BER, while the *General Scheme* has the highest BER. This is because in the *General Scheme*, the dedicated energy signals are transmitted by targeting all the receive antennas. As a result, they impose serious interference on the demodulator in both the conventional and spatial domain. According to the BER comparison between the *Distinct Scheme* and the *Superimposed Scheme*, we observe that the interference on the conventional demodulator has more adverse impact on the demodulation than the interference on the spatial demodulator. Moreover, as illustrated in Fig. 3(a), QPSK outperforms both 8PSK and 16QAM in terms of the BER performance. Observe from Fig. 3(b) that having more receive antennas may increase the BER, since the receiver is more likely to recover the conventional information targeting a wrong receive antenna.

With the same parameter settings as Fig. 2, we plot the energy harvested per symbol versus ISNR by adopting different number of receive antennas in Fig. 4, where we set the symbol duration $T = 10^{-6}s$. Observe from Fig. 4 that the *General Scheme* achieves the highest energy harvesting performance, since the dedicated energy signals target all the receive antennas. Meanwhile, the *Superimposed Scheme* has the lowest energy harvesting performance. Note that in the *Superimposed Scheme*, the energy harvesting performance is uncorrelated to the number of

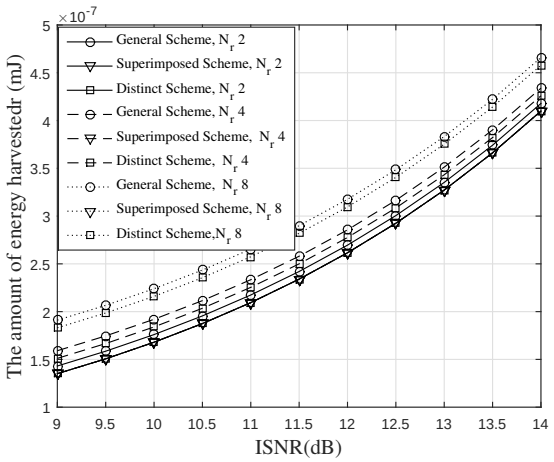


Fig. 4. The amount of energy harvested versus ISNR with different receive antennas number

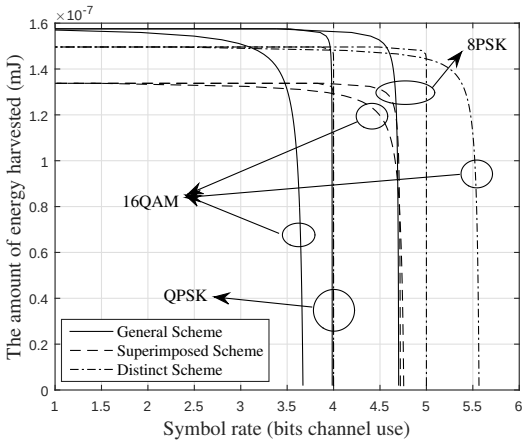


(a) R−E region with different conventional modulators, where $N_r = 4$

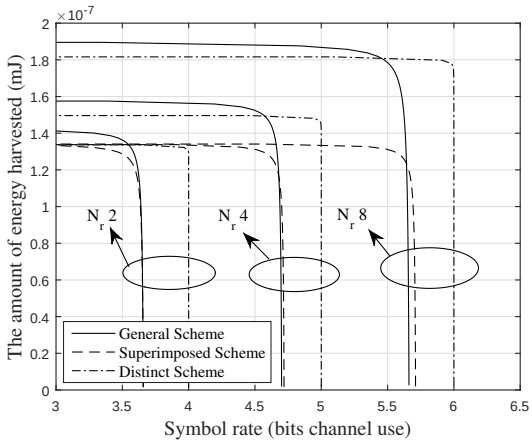


(b) R−E region with different receive antennas number, when 8PSK is adopted in the conventional domain

Fig. 5. R−E region of the RSM-SWIPT system

receive antennas, since the dedicated energy signal always targets a single antenna. By contrast, for the *General Scheme* and the *Distinct Scheme*, the energy harvesting performance increases, when we have more receive antennas.

We then plot the rate-energy (R-E) region in Fig. 5 by changing the power splitting ratio $\rho$ from 0.001 to 0.999, where ISNR is set to 30dB and the variance of energy signal remains unchanged. Observe from Fig. 5(a) that for every transmission scheme, the maximum amount of energy harvested by adopting different conventional modulators is always the same. Moreover, for

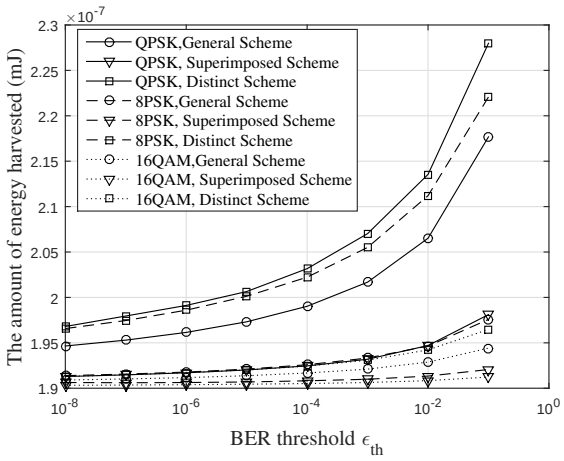


Fig. 6. Energy harvesting power versus BER threshold, where $N_r = 4$

a specific conventional modulator, the *General Scheme* achieves the highest energy harvesting performance but the lowest rate. By contrast, the *Distinct Scheme* achieve the lowest energy harvesting performance but the highest rate. Note that the rate difference between the *General Scheme* and the *Distinct Scheme* becomes larger, when the order of the conventional modulation increases. Another interesting observation is that the *General Scheme* associated with 16QAM has the lowest rate. This is because although the spectrum efficiency of 16QAM is the highest, its BER performance by adopting the *General Scheme* is the poorest, which results in the lowest rate. Furthermore, the impact of the number of receive antennas on the R-E region is investigated in Fig. 5(b). The maximum energy harvesting performance of the *Superimposed Scheme* keeps the same, when different number of receive antennas are conceived. By implementing the *General Scheme* and the *Distinct Scheme*, increasing the number of receive antennas may enlarge the R-E region. Furthermore, as shown in Fig. 5, the *Distinct Scheme* has the largest R-E region. Moreover, the *General Scheme* is the best choice for WPT, when the requirement of the WIT is not very stringent.

### C. Optimal Transceiver Design

We investigate the tradeoff between the maximum WPT performance and the WIT requirement in Fig. 6 by obtaining the near-optimal transceiver design of (P2). As shown in Fig.6, the maximum energy harvested increases, as we relax the BER requirement. Furthermore, observe from Fig.6 that when the BER threshold is fixed, a higher order modulator always achieves a lower WPT performance. This is because that when the signal power $P_s$, the covariance matrix $\mathbf{\Omega}$ of the dedicated energy signal as well as the power splitting ratio $\rho$ is fixed, the WPT performance of modulators having different orders is always the same, according to Eq. (7). However, since the Euclidean distance between the adjacent constellation points is small, a higher order modulator always has a lower BER performance. Therefore, when a lower order modulator is adopted, we could increase the power splitting ratio $\rho$ to obtain the same BER as the higher order one, while the WPT performance is consequently improved. Moreover, the *Distinct Scheme* outperforms its counterparts in terms of the maximum amount of energy harvested, when the BER requirement is fixed.

## VI. Conclusion

In this paper, we studied an RSM aided SWIPT system associated with three different transmission schemes, namely the *General Scheme*, the *Superimposed Scheme* and the *Distinct Scheme*. Various SWIPT performance has been analysed in closed-form. Furthermore, the transceiver is optimised for maximising the WPT performance by finding the optimal covariance matrix of the dedicated energy signals, the transmit power of the modulated information signal and the power splitting ratio, while ensuring various WIT requirements. A number of numerical results validates our theoretical analysis and optimal transceiver design, while demonstrating that the *Distinct Scheme* has the best performance in the RSM aided SWIPT system.

## Appendix A

## Proof of Theorem 1

According to the PEP definition [10], the probability of the original transmit symbol $\mathbf{s}_{m,j}$ being demodulated as $\mathbf{s}_{m,i}$ is then derived as Eq. (32), where $y_{I,j}$ represents the $j$-th element of $\mathbf{y}_I$. Since we have $w_j \sim \mathbb{C}\mathcal{N}(0, (\mathbf{\Omega})_{j,j})$, $z_{a,j} \sim \mathbb{C}\mathcal{N}(0, \sigma_a^2)$ and $z_{\text{cov},j} \sim \mathbb{C}\mathcal{N}(0, \sigma_{\text{cov}}^2)$, while $w_i$, $w_j$, $z_{a,i}$, $z_{a,j}$, $z_{\text{cov},i}$ and $z_{\text{cov},j}$ are independent random variables, the Left-Hand-Side (LHS) of Eq. (32) obeys a Gaussian distribution of $\mathcal{N}(0, P_s|b_m|^2((\mathbf{\Omega})_{i,i}/2 + (\mathbf{\Omega})_{j,j}/2 + \sigma_a^2 + \sigma_{\text{cov}}^2/(1-\rho)))$. Therefore, $\tau_S(\mathbf{s}_{m,j} \to \mathbf{s}_{m,i})$ is derived as Eq. (12).

The probability of the original transmit symbol $\mathbf{s}_{m,j}$ being demodulated as $\mathbf{s}_{n,j}$ is then derived as Eq. (33). Similar to the derivation of Eq. (32), the LHS of Eq. (33) obeys a Gaussian distribution of $\mathcal{N}(0, P_s|b_n - b_m|^2((\mathbf{\Omega})_{j,j}/2 + \sigma_a^2/2 + \sigma_{\text{cov}}^2/2(1-\rho)))$. Therefore, $\tau_C(\mathbf{s}_{m,j} \to \mathbf{s}_{n,j})$ is derived as Eq. (12).

The probability of the original transmit symbol $\mathbf{s}_{m,j}$ being demodulated as $\mathbf{s}_{n,i}$ is then derived as Eq. (34). Similarly, the LHS of (34) obeys a Gaussian distribution of $\mathcal{N}(0, P_s|b_n|^2(\mathbf{\Omega})_{i,i}/2 + P_s|b_m|^2(\mathbf{\Omega})_{j,j}/2 + P_s(|b_n|^2 + |b_m|^2)(\sigma_a^2/2 + \sigma_{\text{cov}}^2/2(1-\rho)))$. Therefore, $\tau_B(\mathbf{s}_{m,j} \to \mathbf{s}_{n,i})$ is derived as Eq. (12).

## Appendix B

## Proof of Theorem 2

For the *General Scheme*, let $P_s^\dagger$, $\mathbf{\Omega}^\dagger$ and $\rho^\dagger$ constitute the optimal solution to (P2), while we have $\|\mathbf{\Lambda}_j\|_2^2 \geq \frac{1}{N_r}\sum_{i=1}^{N_r}\|\mathbf{\Lambda}_i\|_2^2$ and $(\mathbf{\Omega}^\dagger)_{j,j} \neq 0$. The corresponding energy harvesting performance, the transmit power and the BER are denoted by $E_G^\dagger$, $P_t^\dagger$ and $\epsilon_G^\dagger$, respectively. If another solution $\{\rho^\ddagger, P^\ddagger, \mathbf{\Omega}^\ddagger\}$ satisfies $\rho^\ddagger = \rho^\dagger$, $P_s^\ddagger = P_s^\dagger + (\mathbf{\Omega}^\dagger)_{j,j}$, $(\mathbf{\Omega}^\ddagger)_{j,j} = 0$ as well as $(\mathbf{\Omega}^\ddagger)_{i,i} = (\mathbf{\Omega}^\dagger)_{i,i}$ for $i \neq j$,

$$\begin{aligned}
\tau_S(\mathbf{s}_{m,j} \to \mathbf{s}_{m,i}) &= \Pr\left[\|\mathbf{y}_I/\sqrt{1-\rho} - \mathbf{s}_{m,j}\|_2^2 > \|\mathbf{y}_I/\sqrt{1-\rho} - \mathbf{s}_{m,i}\|_2^2\right] \\
&= \Pr\left[P_s|b_m|^2 - 2\mathcal{R}\left(\left(y_{I,j}\right)^* \sqrt{P_s}b_m/\sqrt{1-\rho}\right) > P_s|b_m|^2 - 2\mathcal{R}\left((y_{I,i})^* \sqrt{P_s}b_m/\sqrt{1-\rho}\right)\right] \\
&= \Pr\left[\mathcal{R}\left((y_{I,i})^* \sqrt{P_s}b_m/\sqrt{1-\rho}\right) - \mathcal{R}\left(\left(y_{I,j}\right)^* \sqrt{P_s}b_m/\sqrt{1-\rho}\right) > 0\right] \\
&= \Pr\Big[\mathcal{R}\left(\left(\sqrt{1-\rho}(w_i + z_{a,i}) + z_{\text{cov},i}\right)^* \sqrt{P_s}b_m/\sqrt{1-\rho}\right) \\
&\quad -\mathcal{R}\left(\left(\sqrt{1-\rho}(\sqrt{P_s}b_m + w_j + z_{a,j}) + z_{\text{cov},j}\right)^* \sqrt{P_s}b_m/\sqrt{1-\rho}\right) > 0\Big] \\
&= \Pr\left[\underbrace{\mathcal{R}\left(\sqrt{P_s}b_m^*\left(w_i - w_j + z_{a,i} - z_{a,j} + (z_{\text{cov},i} - z_{\text{cov},j})/\sqrt{1-\rho}\right)\right)}_{LHS} > P_s|b_m|^2\right]. \qquad (32)
\end{aligned}$$

$$\begin{aligned}
\tau_C(\mathbf{s}_{m,j} \to \mathbf{s}_{n,j}) &= \Pr\left[\|\mathbf{y}_I/\sqrt{1-\rho} - \mathbf{s}_{m,j}\|_2^2 > \|\mathbf{y}_I/\sqrt{1-\rho} - \mathbf{s}_{n,j}\|_2^2\right] \\
&= \Pr\left[P_s|b_m|^2 - 2\mathcal{R}\left((y_{I,j})^* \sqrt{P_s}b_m/\sqrt{1-\rho}\right) > P_s|b_n|^2 - 2\mathcal{R}\left((y_{I,j})^* \sqrt{P_s}b_n/\sqrt{1-\rho}\right)\right] \\
&= \Pr\left[\mathcal{R}\left((y_{I,j})^* \sqrt{P_s}b_n/\sqrt{1-\rho}\right) - \mathcal{R}\left((y_{I,j})^* \sqrt{P_s}b_m/\sqrt{1-\rho}\right) > P_s(|b_n|^2 - |b_m|^2)/2\right] \\
&= \Pr\Big[\mathcal{R}\left((\sqrt{1-\rho}(\sqrt{P_s}b_m + w_j + z_{a,j}) + z_{\text{cov},j})^* \sqrt{P_s}b_n/\sqrt{1-\rho}\right) \\
&\quad -\mathcal{R}\left((\sqrt{1-\rho}(\sqrt{P_s}b_m + w_j + z_{a,j}) + z_{\text{cov},j})^* \sqrt{P_s}b_m/\sqrt{1-\rho}\right) > P_s(|b_n|^2 - |b_m|^2)/2\Big] \\
&= \Pr\left[\underbrace{\mathcal{R}\left(\sqrt{P_s}(b_n^* - b_m^*)\left(w_j + z_{a,j} + z_{\text{cov},j}/\sqrt{1-\rho}\right)\right)}_{LHS} > P_s(|b_m|^2 + |b_n|^2)/2 - \mathcal{R}(P_s b_m^* b_n)\right]. \qquad (33)
\end{aligned}$$

$$\begin{aligned}
\tau_B(\mathbf{s}_{m,j} \to \mathbf{s}_{n,i}) &= \Pr\left[\|\mathbf{y}_I/\sqrt{1-\rho} - \mathbf{s}_{m,j}\|_2^2 > \|\mathbf{y}_I/\sqrt{1-\rho} - \mathbf{s}_{n,i}\|_2^2\right] \\
&= \Pr\left[P_s|b_m|^2 - 2\mathcal{R}\left((y_{I,j})^* \sqrt{P_s}b_m/\sqrt{1-\rho}\right) > P_s|b_n|^2 - 2\mathcal{R}\left((y_{I,i})^* \sqrt{P_s}b_n/\sqrt{1-\rho}\right)\right] \\
&= \Pr\left[\mathcal{R}\left((y_{I,i})^* \sqrt{P_s}b_n/\sqrt{1-\rho}\right) - \mathcal{R}\left((y_{I,j})^* \sqrt{P_s}b_m/\sqrt{1-\rho}\right) > P_s(|b_n|^2 - |b_m|^2)/2\right] \\
&= \Pr\Big[\mathcal{R}\left((\sqrt{1-\rho}(w_i + z_{a,i}) + z_{\text{cov},i})^* \sqrt{P_s}b_n/\sqrt{1-\rho}\right) \\
&\quad -\mathcal{R}\left((\sqrt{1-\rho}(\sqrt{P_s}b_m + w_j + z_{a,j}) + z_{\text{cov},j})^* \sqrt{P_s}b_m/\sqrt{1-\rho}\right) > P_s(|b_n|^2 - |b_m|^2)/2\Big] \\
&= \Pr\left[\underbrace{\mathcal{R}\left(\sqrt{P_s}b_n^*(w_i + z_{a,i} + \frac{z_{\text{cov},i}}{\sqrt{1-\rho}}) - \sqrt{P_s}b_m^*(w_j + z_{a,j} + \frac{z_{\text{cov},j}}{\sqrt{1-\rho}})\right)}_{LHS} > \frac{P_s(|b_n|^2 + |b_m|^2)}{2}\right]. \qquad (34)
\end{aligned}$$

by substituting $\{\rho^{\ddagger}, P^{\ddagger}, \mathbf{\Omega}^{\ddagger}\}$ to Eq. (7), the energy harvested by the receiver can be calculated as

$$\begin{aligned} E_G^{\ddagger} &= \xi\rho(P_s^{\ddagger} + \mathrm{Tr}(\mathbf{\Omega}^{\ddagger})) + \xi\rho N_r\sigma_a^2 \\ &= \xi\rho(P_s^{\dagger} + (\mathbf{\Omega}^{\dagger})_{j,j} + \mathrm{Tr}(\mathbf{\Omega}^{\dagger}) - (\mathbf{\Omega}^{\dagger})_{j,j}) + \xi\rho N_r\sigma_a^2 \\ &= E_G^{\dagger}. \end{aligned} \tag{35}$$

Moreover, by letting $\mathbf{\Omega}^{\Delta} = \mathbf{\Omega}^{\dagger} - \mathbf{\Omega}^{\ddagger}$, the transmit power at the transmitter is calculated as

$$\begin{aligned} P_t^{\ddagger} =& \frac{1}{N_r} P_s^{\ddagger}\mathrm{tr}(\mathbf{\Lambda}\mathbf{\Lambda}^*) + \mathrm{tr}(\mathbf{\Lambda}\mathbf{\Omega}^{\ddagger}\mathbf{\Lambda}^*) \\ =& \frac{1}{N_r}(P_s^{\dagger} + (\mathbf{\Omega}^{\dagger})_{j,j})\mathrm{tr}(\mathbf{\Lambda}\mathbf{\Lambda}^*) + \mathrm{tr}(\mathbf{\Lambda}(\mathbf{\Omega}^{\dagger} - \mathbf{\Omega}^{\Delta})\mathbf{\Lambda}^*) \\ =& P_t^{\dagger} + \frac{1}{N_r}(\mathbf{\Omega}^{\dagger})_{j,j}\mathrm{tr}(\mathbf{\Lambda}\mathbf{\Lambda}^*) - \mathrm{tr}(\mathbf{\Lambda}\mathbf{\Omega}^{\Delta}\mathbf{\Lambda}^*) \\ =& P_t^{\dagger} + (\mathbf{\Omega}^{\dagger})_{j,j}\left(\frac{1}{N_r}\sum_{i=1}^{N_r} \|\mathbf{\Lambda}_i\|_2^2 - \|\mathbf{\Lambda}_j\|_2^2\right) \\ \leq& P_t^{\dagger} \leq P_{\max}. \end{aligned} \tag{36}$$

Furthermore, since we have $\rho^{\ddagger} = \rho^{\dagger}$, $P_s^{\ddagger} > P_s^{\dagger}$ and $(\mathbf{\Omega}^{\ddagger})_{j,j} < (\mathbf{\Omega}^{\dagger})_{j,j}$, the BER of the new solution must satisfy $\epsilon_G^{\ddagger} < \epsilon_G^{\dagger} \leq \epsilon_{\mathrm{th}}^{'}$.

Therefore, $\{\rho^{\ddagger}, P_s^{\ddagger}, \mathbf{\Omega}^{\ddagger}\}$ achieves the same energy harvested with its counterpart $\{\rho^{\dagger}, P_s^{\dagger}, \mathbf{\Omega}^{\dagger}\}$, while its BER performance is lower than the requirement $\epsilon_{\mathrm{th}}^{'}$. Therefore, we may increase $\rho^{\ddagger}$ until we have $\epsilon_G^{\ddagger} = \epsilon_{\mathrm{th}}^{'}$, while the energy harvested is consequently increased to be higher than $E_G^{\dagger}$. This result indicates that $\{\rho^{\dagger}, P^{\dagger}, \mathbf{\Omega}^{\dagger}\}$ is not the optimal solution, which violates the assumption. As a result, when the solution achieves optimality, the covariance matrix of the dedicated energy signal has to satisfy $(\mathbf{\Omega})_{j,j} = 0$, if we have $\|\mathbf{\Lambda}_j\|_2^2 \geq \frac{1}{N_r}\sum_{i=1}^{N_r}\|\mathbf{\Lambda}_i\|_2^2$ , for $\forall j = 1, \cdots, N_r$.

Similar proofs can be obtained by letting $P_s^{\ddagger} = P_s^{\dagger} + \frac{1}{N_r}(\mathbf{\Omega}^{\dagger})_{j,j}$ for the *Superimposed Scheme*, and $P^{\ddagger} = P^{\dagger} + \frac{N_r-1}{N_r}(\mathbf{\Omega}^{\dagger})_{j,j}$ for the *Distinct Scheme*.

## Appendix C
## Proof of Theorem 3

At first, the objective function of (P5) is re-grouped as $\log(E) = f(\mu) + g\left(P_s, \{(\mathbf{\Omega})_{j,j}\}\right)$, where $f(\mu) = \log(\xi T) + \log(\frac{\mu-1}{\mu})$ and $g\left(P_s, \{(\mathbf{\Omega})_{j,j}\}\right) = \log(P_s + \sum_{j=1}^{N_r}(\mathbf{\Omega})_{j,j} + N_r\sigma_a^2)$. We then prove the concavity of $f(\cdot)$ and that of $g(\cdot)$, respectively.

- *$f(\cdot)$ is a concave function w.r.t. $\mu$.* The second-order derivative of $f(\mu)$ is derived as

$$\frac{\partial^2 f}{\partial \mu^2} = \left(\frac{1}{\mu^2} - \frac{1}{(\mu-1)^2}\right). \tag{37}$$

  Since $\rho$ is lower than 1, we have $\mu > 1$ and $\frac{\partial^2 f}{\partial \mu^2} < 0$.

- *$g(\cdot)$ is a concave function w.r.t. $P_s$ and $\{\{(\mathbf{\Omega})_{j,j}|j = 1, \cdots, N_r\}\}$.* In order to improve the readability, we substitute $P_s$ by the notation $x_1$, and substitute $\{(\mathbf{\Omega})_{j,j}|j = 1, \cdots, N_r\}$ by the notations $\{x_{j+1}|j = 1, \cdots, N_r\}$. Therefore, the function $g(\cdot)$ is reformulated as $g(x_1, \cdots, x_{N_r+1}) = \log(\sum_{i=1}^{N_r+1} x_i + N_r\sigma_a^2)$, where the Hessian matrix of the function $g(x_1, \cdots, x_{N_r+1})$ is expressed as

$$G = \begin{bmatrix} \frac{\partial^2 g}{\partial x_1^2} & \cdots & \frac{\partial^2 g}{\partial x_1 \partial x_{N_r+1}} \\ \vdots & \ddots & \vdots \\ \frac{\partial^2 g}{\partial x_{N_r+1}\partial x_1} & \cdots & \frac{\partial^2 g}{\partial x_{N_r+1}\partial x_{N_r+1}} \end{bmatrix}, \tag{38}$$

  where $\frac{\partial^2 g}{\partial x_i \partial x_j} = -\frac{1}{(\sum_{i'=1}^{N_r+1} x_{i'} + N_r\sigma_a^2)^2}$ for $i = 1, \cdots, N_r + 1$ and $j = 1, \cdots, N_r + 1$. Obviously $G$ is a non-positive definite matrix, which indicates the concavity of $g(x_1, \cdots, x_{N_r+1})$.

- Since both $f(\cdot)$ and $g(\cdot)$ are concave functions w.r.t. $P_s$, $\{(\mathbf{\Omega})_{j,j}|j = 1, \cdots, N_r\}$ and $\mu$, their summation $\log(E)$ is also concave w.r.t. these variables. Moreover, (30a)-(30d) of (P5) are linear constraints w.r.t. $P_s$, $\{(\mathbf{\Omega})_{j,j}|j = 1, \cdots, N_r\}$ and $\mu$. As a result, (P5) is a concave optimisation problem.

## REFERENCES


[1] A. Al-Fuqaha, M. Guizani, M. Mohammadi, M. Aledhari, and M. Ayyash, "Internet of things: A survey on enabling technologies, protocols, and applications," *IEEE Communications Surveys Tutorials*, vol. 17, no. 4, pp. 2347 – 2376, 2015.

[2] K. Zheng, L. Zhao, J. Mei, B. Shao, W. Xiang, and L. Hanzo, "Survey of large-scale MIMO systems," *IEEE Communications Surveys Tutorials*, vol. 17, no. 3, pp. 1738 – 1760, 2015.

[3] L. Zhang, Y. Li, and L. J. Cimini, "Statistical performance analysis for MIMO beamforming and STBC when co-channel interferers use arbitrary MIMO modes," *IEEE Transactions on Communications*, vol. 60, no. 10, pp. 2926–2937, October 2012.

[4] E. Basar, M. Wen, R. Mesleh, M. D. Renzo, Y. Xiao, and H. Haas, "Index modulation techniques for next-generation wireless networks," *IEEE Access*, vol. 5, pp. 16 693 – 16 746, 2017.

[5] E. Basar, "Index modulation techniques for 5G wireless networks," *IEEE Communications Magazine*, vol. 54, no. 7, pp. 168–175, July 2016.

[6] M. D. Renzo, H. Haas, A. Ghrayeb, S. Sugiura, and L. Hanzo, "Spatial modulation for generalized MIMO: Challenges, opportunities, and implementation," *Proceedings of the IEEE*, vol. 102, no. 1, pp. 56–103, Jan 2014.

[7] L. He, J. Wang, and J. Song, "Spatial modulation for more spatial multiplexing: RF-chain-limited generalized spatial modulation aided MM-Wave MIMO with hybrid precoding," *IEEE Transactions on Communications*, vol. 66, no. 3, pp. 986–998, March 2018.

[8] N. Ishikawa, S. Sugiura, and L. Hanzo, "50 years of permutation, spatial and index modulation: From classic RF to visible light communications and data storage," *IEEE Communications Surveys Tutorials*, vol. 20, no. 3, pp. 1905–1938, thirdquarter 2018.

[9] X. zhu, Z. Wang, and J. Cao, "NOMA-based spatial modulation," *IEEE Access*, vol. 5, pp. 3790–3800, 2017.

[10] R. Zhang, L. Yang, and L. Hanzo, "Generalised pre-coding aided spatial modulation," *IEEE Transactions on Wireless Communications*, vol. 12, no. 11, pp. 5434–5443, November 2013.

[11] T. A. Khan, A. Yazdan, and R. W. Heath, "Optimization of power transfer efficiency and energy efficiency for wireless-powered systems with massive MIMO," *IEEE Transactions on Wireless Communications*, vol. 17, no. 11, pp. 7159–7172, Nov 2018.

[12] X. Zhou, R. Zhang, and C. K. Ho, "Wireless information and power transfer in multiuser OFDM systems," *IEEE Transactions on Wireless Communications*, vol. 13, no. 4, pp. 2282–2294, April 2014.

[13] S. Guo, H. Zhang, Y. Wang, and D. Yuan, "Spatial modulated simultaneous wireless information and power transfer," in *2016 IEEE Global Communications Conference (GLOBECOM)*, Dec 2016, pp. 1–6.

[14] C. Liu, M. Ma, Y. Yang, and B. Jiao, "Optimal spatial-domain design for spatial modulation capacity maximization," *IEEE Communications Letters*, vol. 20, no. 6, pp. 1092–1095, June 2016.

[15] P. S. Koundinya, K. V. S. Hari, and L. Hanzo, "Joint design of the spatial and of the classic symbol alphabet improves single-RF spatial modulation," *IEEE Access*, vol. 4, pp. 10 246–10 257, 2016.

[16] X. Zhou, L. Yang, C. Wang, and D. Yuan, "SCM-SM: Superposition coded modulation-aided spatial modulation with a low-complexity detector," *IEEE Transactions on Vehicular Technology*, vol. 63, no. 5, pp. 2488–2493, Jun 2014.

[17] X. Wu, M. D. Renzo, and H. Haas, "Adaptive selection of antennas for optimum transmission in spatial modulation," *IEEE Transactions on Wireless Communications*, vol. 14, no. 7, pp. 3630–3641, July 2015.

[18] C. Zhong, X. Hu, X. Chen, D. W. K. Ng, and Z. Zhang, "Spatial modulation assisted multi-antenna non-orthogonal multiple access," *IEEE Wireless Communications*, vol. 25, no. 2, pp. 61–67, April 2018.

[19] R. Zhang, L. Yang, and L. Hanzo, "Error probability and capacity analysis of generalised pre-coding aided spatial modulation," *IEEE Transactions on Wireless Communications*, vol. 14, no. 1, pp. 364–375, Jan 2015.

[20] J. Hu, K. Yang, G. Wen, and L. Hanzo, "Integrated data and energy communication network: A comprehensive survey," *IEEE Communications Surveys Tutorials*, vol. 20, no. 4, pp. 3169–3219, Fourthquarter 2018.

[21] K. Lv, J. Hu, Q. Yu, and K. Yang, "Throughput maximization and fairness assurance in data and energy integrated communication networks," *IEEE Internet of Things Journal*, vol. 5, no. 2, pp. 636–644, April 2018.

[22] D. Wang, R. Zhang, X. Cheng, and L. Yang, "Capacity-enhancing full-duplex relay networks based on power-splitting (PS-)SWIPT," *IEEE Transactions on Vehicular Technology*, vol. 66, no. 6, pp. 5445–5450, June 2017.

[23] Y. Zhao, J. Hu, Y. Diao, Q. Yu, and K. Yang, "Modelling and performance analysis of wireless LAN enabled by RF energy transfer," *IEEE Transactions on Communications*, vol. 66, no. 11, pp. 5756–5772, Nov 2018.

[24] J. Hu, Y. Zhao, and K. Yang, "Modulation and coding design for simultaneous wireless information and power transfer," *IEEE Communications Magazine*, vol. 57, no. 5, pp. 124–130, May 2019.

[25] Y. Zhao, J. Hu, Z. Ding, and K. Yang, "Joint interleaver and modulation design for multi-user SWIPT-NOMA," *IEEE Transactions on Communications*, pp. 1–1, 2019.

[26] M. Zhang and X. Cheng, "Spatial-modulation-based wireless-powered communication for achievable rate enhancement," *IEEE Communications Letters*, vol. 21, no. 6, pp. 1365–1368, June 2017.

[27] R. Zhang, L. Yang, and L. Hanzo, "Energy pattern aided simultaneous wireless information and power transfer," *IEEE Journal on Selected Areas in Communications*, vol. 33, no. 8, pp. 1492–1504, Aug 2015.

[28] C. Cheng, M. D. Renzo, F. Graziosi, and A. Zappone, "On simultaneous wireless information and power transfer for receive spatial modulation," *IEEE Access*, vol. 5, pp. 23 204–23 211, 2017.

[29] M. Li, I. B. Collings, S. V. Hanly, C. Liu, and P. Whiting, "Multicell coordinated scheduling with multiuser zero-forcing beamforming," *IEEE Transactions on Wireless Communications*, vol. 15, no. 2, pp. 827–842, Feb 2016.

[30] S. Boyd and L. Vandenberghe, *Convex Optimization*, 2004.